MINERALOGY OF THE MERCURIAN SURFACE. Kathleen E. Vander Kaaden[1,2], Francis M. McCubbin[1,2], Larry R. Nittler[3], Patrick N. Peplowski[4], Shoshana Z. Weider[3], Larry R. Evans[5], Elizabeth A. Frank[3], Timothy McCoy[6]. [1]Institute of Meteoritics, Department of Earth and Planetary Sciences, 1 University of New Mexico, MSC03-2050, Albuquerque, NM 87131. [2]NASA Johnson Space Center, Mailcode XI2, 2101 NASA Parkway, Houston, TX 77058. [3]Department of Terrestrial Magnetism, Carnegie Institution of Washington, Washington, DC 20015. [4]The Johns Hopkins University Applied Physics Laboratory, Laurel, MD 20723. [5]Computer Science Corporation, Lanham-Seabrook, MD 20706. [6]Smithsonian Institution, Washington, DC 20560, (kvander@unm.edu).

Introduction: The MErcury Surface, Space ENvironment, GEochemistry, and Ranging (MESSENGER) spacecraft orbited Mercury for four years until April 2015, revealing its structure, chemical makeup, and compositional diversity. Data from the mission have confirmed that Mercury is a compositional end-member among the terrestrial planets [1]. The X-Ray Spectrometer (XRS) and Gamma-Ray Spectrometer (GRS) on board MESSENGER provided the first detailed geochemical analyses of Mercury's surface [e.g., 2–5]. These instruments have been used in conjunction with the Neutron Spectrometer and the Mercury Dual Imaging System to classify numerous geological and geochemical features on the surface of Mercury that were previously unknown. Furthermore, the data have revealed several surprising characteristics about Mercury's surface, including elevated S abundances (up to 4 wt%) and low Fe abundances (less than 2.5 wt%) [3, 6]. The S and Fe abundances were used to quantify Mercury's highly reduced state, i.e., between 2.6 and 7.3 $\log_{10}$ units below the Iron-Wüstite (IW) buffer [7, 8]. This fO_2 is lower than any of the other terrestrial planets in the inner Solar System [9–11] and has important consequences for the thermal and magmatic evolution of Mercury, its surface mineralogy and geochemistry, and the petrogenesis of the planet's magmas [3, 7, 12–16]. Although MESSENGER has revealed substantial geochemical diversity across the surface of Mercury, until now, there have been only limited efforts to understand the mineralogical and petrological diversity of the planet [13, 14, 16]. Here we present a systematic and comprehensive study of the potential mineralogical and petrological diversity of Mercury.

Methods: We focus our study on nine regions (Figure 1) with characteristic major element compositions [6]: (i) the high-Mg region (HMR), (ii) a sub-region of the HMR with the planet's highest Ca and S contents (HMR-CaS), (iii) the smooth plains within the Caloris basin (CB), (iv) a subset of the northern volcanic plains (NP) with relatively high Mg content (NP-HMg), (v) a subset of the NP with relatively low Mg content (NP-LMg), (vi) the Rachmaninoff basin (RB), (vii) the high-Al regions southwest and southeast of the NP (HAl), (viii) the planet's largest pyroclastic deposit, located northeast of the Rachmaninoff basin (PD), and (ix) the intermediate terrane (IT), made up of intercratered plains and highly-cratered terrain. We have used modified average compositions for these geochemical regions defined in [17] to compute the normative mineralogy of the mercurian surface. For each composition, two normative compositions were calculated: 1) using only the measured Cr, Mn, and Ti from XRS and 2) using the XRS detection limits of Cr, Mn, and Ti reported in [3] as upper limit values for these three elements. Due to the high amount of sulfur in mercurian compositions, the CIPW normative mineralogy calculations could not be conducted in the conventional manner. Instead, we first calculated the sulfides that would be present in each composition using partition coefficients from [16], which were determined for Mercury-relevant compositions and fO_2 conditions. These data indicate that S bonds with Fe, Cr, Ti, Mn, Mg, and Ca, respectively, listed in descending order of preference. Once all the S is consumed as sulfides, the composition is renormalized with these components removed to produce a S-free composition. We then used this composition to calculate the normative mineralogy of each geochemical region following the steps of [18]. A modification that we made to this classical calculation was the treatment of MnO. Typically, MnO is assumed to act like FeO. Given the highly reducing nature of Mercury [7, 8], however, as well as the low amount of Fe and Ti on the surface [3, 19], we have elected to force all Mn that is left after making MnS into a manganosite component (MnO). The resulting compositions are given in Table 1.

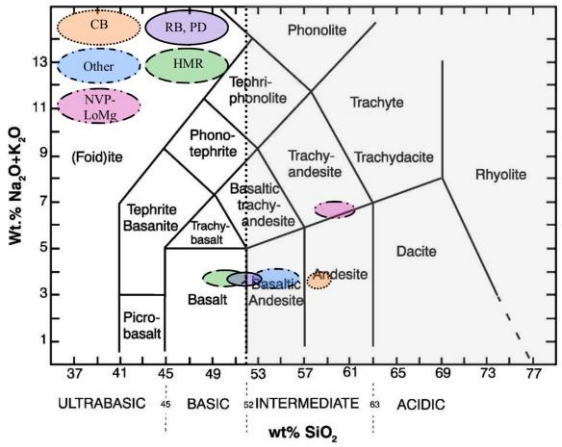

Figure 1. *Total alkali versus silica (TAS) diagram for nine distinct geochemical units on Mercury. Dotted line is at 52 wt% SiO_2. Shaded region >52 wt% SiO_2 represents boninites. Unshaded region <52 wt% SiO_2 represents komatiitic compositions.*

Table 1. *CIPW norm calculations (wt%) for each of the distinct geochemical regions. Detection limits for Cr, Mn, and Ti from [3] are used as upper limit values for these elements.*

	HMR	HMR-CaS	CB	NP-HMg	NP-LMg	RB	HAl	PD	IT
FeS	2.38	2.61	1.19	2.41	1.84	2.32	1.16	0.21	2.20
CrS	0.76	0.74	0.88	0.81	0.85	0.77	0.82	0.00	0.82
TiS_2	1.66	1.62	0.63	0.98	1.85	1.68	1.77	0.00	1.13
MnS	0.75	0.73	0.86	0.00	0.27	0.76	0.21	0.00	0.00
MgS	0.36	0.75	0.07	0.00	0.00	0.20	0.00	0.00	0.00
CaS	0.03	0.08	0.01	0.00	0.00	0.02	0.00	0.00	0.00
Quartz	0.00	0.00	6.12	0.00	0.00	0.00	0.00	0.00	0.00
Plagioclase	40.21	32.42	57.53	46.63	57.34	41.28	57.38	45.30	50.95
Orthoclase	0.95	0.95	0.53	1.42	1.06	0.95	0.95	0.96	0.65
Nepheline	0.00	3.10	0.00	0.00	0.00	0.00	0.00	0.00	0.00
Corundum	0.00	0.00	0.28	0.00	0.00	0.00	0.25	0.00	0.00
Diopside	18.04	22.43	0.00	6.30	18.29	16.67	0.00	16.77	3.80
Hypersthene	0.28	0.00	31.91	23.51	9.26	4.04	30.02	3.59	31.49
Olivine	34.59	34.58	0.00	15.95	8.74	31.34	6.99	31.36	7.17
Ilmenite	0.00	0.00	0.00	0.00	0.00	0.00	0.00	1.18	0.00
Sphene	0.00	0.00	0.00	1.35	0.00	0.00	0.00	0.00	1.13
MnO	0.00	0.00	0.00	0.65	0.48	0.00	0.48	0.63	0.66

Results: Our resultant mineralogy (Table 1) of the mercurian surface includes FeS (0.21–2.68 wt%), CrS (0–0.88 wt%), TiS_2 (0–1.85 wt%), MnS (0–0.86 wt%), MgS (0–3.23 wt%), CaS (0–0.33 wt%), quartz (0–7.90 wt%), plagioclase (32.42–58.35 wt%), orthoclase (0.53–1.42 wt%), nepheline (0–3.10 wt%), corundum (0–0.80 wt%), hypersthene (0–37.13 wt%), diopside (0–37.13 wt%), olivine (0–34.59 wt%), ilmenite (0–1.18 wt%), sphene (0–1.35 wt%), and MnO (0–0.66 wt%). Plagioclase is the dominant mineral across all geochemical regions, consistent with the results of [4, 14]. All compositions are hypersthene normative with the exception of the HMR-CaS, which is slightly nepheline normative (3.1%). This difference in normative mineralogy could have implications for the degree of homogenization of the mantle, as well as the petrogenetic processes that produced the geochemically diverse surface. By including the detection limits of Cr, Mn, and Ti into the oxide composition, minor CrS, MnS, ilmenite, sphene, and MnO are produced, which would not otherwise be present. The abundances of these components should be considered maximum possible values.

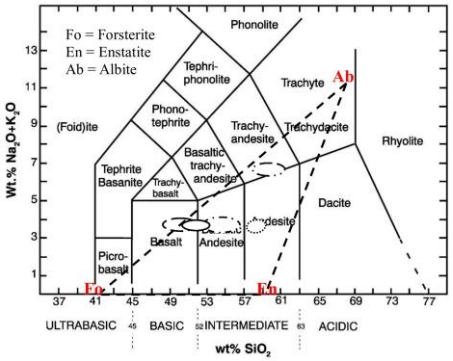

Figure 2. *TAS diagram containing end member minerals forsterite (Fo), enstatite (En), and Albite (Ab). Fields for Mercury's geochemical regions are the same as in Figure 1.*

Discussion: Our results indicate that Mercury's surface possesses a diverse set of rocks, with a wide range of SiO_2 content, alkali content, and major element compositions. The compositional diversity of these nine geochemical regions likely results in a diverse surface mineralogy, as indicated by CIPW norm calculations (Table 1). The primary mineralogy of the surface rocks, however, are likely dominated by forsterite, enstatite, and albitic plagioclase, as indicated by all the compositions falling within a forsterite-enstatite-albite triangle on a TAS diagram (Fig. 2).

The olivine-normative nature of the surface is an important finding because it indicates that enstatite chondrites and aubrites may not be as good as petrologic analogs for Mercury as previously thought [3, 20]. These meteorites are dominated by enstatite (with only minor olivine), whereas the Mercury's surface compositions, partly because of their Na-rich nature, are highly forsterite normative. Phase equilibrium studies also indicate olivine-rich mantle sources on Mercury.

References: [1] Solomon S. C. et al. (2001) *PSS, 49*, 1445–1465. [2] Evans L. G. et al. (2012) *JGR Planets, 117*, E00L07. [3] Nittler L. R. et al. (2011) *Science, 333*, 1847–1850. [4] Peplowski P. N. et al. (2014) *Icarus, 228*, 86–95. [5] Weider S. Z. et al. (2012) *JGR Planets, 117*, E00L05. [6] Weider S. Z. et al. (2015) *EPSL, 416*, 109–120. [7] McCubbin F. M. et al. (2012) *GRL, 39*, L09202. [8] Zolotov M. Y. et al. (2013) *JGR Planets, 118*, 138–146. [9] Herd C. D. K. (2008) *Rev. Mineral. Geochem., 68*, 527–553. [10] Sharp Z. D. et al. (2013) *EPSL, 380*, 88–97. [11] Wadhwa M. (2008) *Rev. Mineral. Geochem., 68*, 493–510. [12] Brown S. M. and Elkins-Tanton L. T. (2009) *EPSL, 286*, 446–455. [13] Charlier B. et al. (2013) *EPSL, 363*, 50–60. [14] Stockstill-Cahill K. R. et al. (2012) *JGR Planets, 117*, E00L15. [15] Vander Kaaden K. E. and McCubbin F. M. (2015) *JGR Planets, 120*, 195–209. [16] Vander Kaaden K. E. and McCubbin F. M. (2016) *GCA, 173*, 246–263. [17] Vander Kaaden K. E. et al. (2015) *LPS, 46*, Abstract #1364. [18] Johannsen A. (1931) A descriptive petrography of the igneous rocks in University of Chicago Press. (1931), vol. 1, pp. 88–92. [19] Weider S. Z. et al. (2014) *Icarus, 235*, 170–186. [20] Burbine T. H. et al. (2002) Meteorit. Planet. Sci., 37, 1233–1244.